

# Structural Relaxation Dynamics of *ortho*-Terphenyl

C.M. ROLAND and K.L. NGAI

*Naval Research Laboratory, Washington, DC 20375-5320, U.S.A.*

(Received 16 October 1996; accepted in revised form 20 May 1997)

**Abstract.** This paper analyzes molecular dynamics simulation results on the small-molecule glass former *ortho*-terphenyl (OTP). The data can be described well using the coupling model of relaxation. The dynamic susceptibility calculated from the density-density time correlation function is shown to approximately conform to the scaling laws of mode coupling theory. Since the dynamic singularities of mode coupling theory are absent in the coupling model, both approaches to high frequency structural relaxation cannot be correct; the conformance to mode coupling theory indicates the non-uniqueness of mode coupling theory interpretation of data from fragile liquids. The non-cooperative relaxation time for density fluctuations in OTP is found to have the same activation energy as the shear viscosity in the high temperature limit. This illustrates the relationship between microscopic dynamic variables and the short time behavior of macroscopic properties, when the former are analyzed according to the coupling model.

**Key words:** coupling model, density fluctuations, mode coupling theory, molecular dynamics simulation, *ortho*-terphenyl, phonons, relaxation, viscosity

## Introduction

The two models most often employed to interpret the high frequency/short time dynamics of glass forming liquids and polymers are mode coupling theory (Götze, 1991; Götze and Sjögren 1992) and the coupling model (Ngai, 1994; Ngai and Plazek, 1995; Tsang and Ngai, 1996; Roland and Ngai, 1995, 1997; Ngai and Roland, 1996). The application of mode coupling theory is presently limited to very fast (ca. picosecond) dynamics, whereas the coupling model has more often been utilized to address relaxation at long times (macroscopic behavior). The most important distinction between the two models concerns the existence of critical phenomena; i.e., dynamic singularities. Mode coupling theory, based on non-linear coupling of density fluctuations in condensed matter, predicts a dynamical singularity, and consequent ergodic to non-ergodic transition, at a temperature lying *above* the conventional glass transition temperature,  $T_g$ . The coupling model, on the other hand, lacks any such critical phenomena, rather asserting only that the relaxation rate slows down at times on the order of picosecond due to the influence of intermolecular constraints.

In this paper we fit the coupling model to molecular dynamics simulations on OTP (Lewis and Wahnström, 1994; Roland et al. 1995), to demonstrate that the model can describe such results. Next, we analyze the data according to the prescriptions of mode coupling theory, in order to determine whether features predicted

by mode coupling theory are present in data generated from the coupling model. Finally, in an attempt to make a connection between microscopic and macroscopic properties, we compare the temperature dependence of the non-cooperative relaxation time of the coupling model, as deduced from analyzing the OTP data, with the limiting, high temperature viscosity behavior of OTP.

## Results

### COUPLING MODEL ANALYSIS

Especially at low temperature, vibrational motions contribute to the short time dynamics. Neither the coupling model nor mode coupling theory address these vibrational motions; hence, in the study of relaxations at low temperature, vibrational contributions must be introduced *ad hoc*. One assumption is that the relaxation and the phonon dynamics are independent, whereby the density-density correlation function can be expressed as the product of a vibrational and a relaxation correlation function

$$C(t; Q, T) = C_{\text{pho}}(t; Q, T) \times C_{\text{rel}}(t; Q, T), \quad (1)$$

in which  $Q$  is the wave vector (momentum transfer) and  $T$  the temperature. The phonon contribution  $C_{\text{pho}}(t; Q, T)$  is determined by the density of states of the phonon normal modes (i.e., vibrational spectrum) (Kittel, 1963)

$$C_{\text{pho}}(t; \mathbf{Q}, T) = \exp(-\mathbf{Q}^2 W(t, T)), \quad (2)$$

where, if the phonons are harmonic throughout the temperature region of interest,

$$W(t, T) = KT^2 \int g(\omega) [1 - \cos(\omega t)] \omega^{-1} \left[ \frac{2}{\exp(\hbar\omega/kT)} + 1 \right] d\omega, \quad (3)$$

where  $g(\omega)$  is the frequency spectrum of the normal modes and  $K$  represents a collection of constants.  $W(t, T)$  decreases monotonically with time, leveling off to a constant value. Correspondingly, at long time  $C_{\text{pho}}(t \rightarrow \infty; Q, T)$  assumes the value  $\exp(-Q^2 W(T))$ , which is the well-known Debye–Waller factor (DWF). To calculate the phonon contribution to the measured correlation function requires determination of the phonon density of states. As a crude approximation, a Debye spectrum (Kittel, 1963) can be employed,

$$g_D(\omega) \sim \omega^2, \quad \omega < \omega_D, \quad (4)$$

where  $g_D(\omega) = 0$  for  $\omega > \omega_D$ . A temperature-invariant Debye frequency,  $\omega_D$ , is consistent with simulation data (Lewis and Wahnström, 1994). The abrupt cut-off at  $\omega_D$  leads to unreal oscillations at a few picoseconds in the correlation function, which are eliminated by smoothing (Roland and Ngai, 1995; Roland et al., 1995)

$$g_D(\omega) \sim \omega^2 \exp\left(-\frac{\omega}{\omega_D}\right). \quad (5)$$

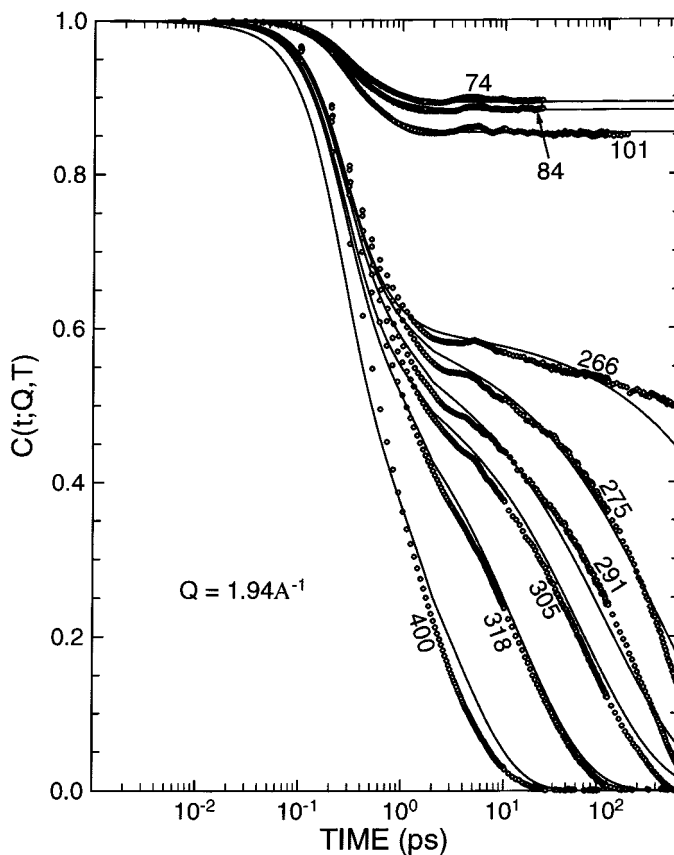


Figure 1. Density-density correlation function for OTP; solid lines are the fits of Equations (1–8) to the molecular dynamics simulation results (Lewis and Wahnström, 1994; Roland et al., 1995). At the three lowest temperatures, there is no relaxation over this time scale.

At low temperature (well below  $T_g = 243$  K), no relaxation occurs over the time scale of the molecular dynamics simulation data, so that  $C_{\text{rel}}(t; Q, T)$  remains unity. The vibrational correlation function in Equation (1) is thus isolated from the relaxational component, and  $C_{\text{pho}}(t; Q, T, )$  can be determined from fitting the OTP data for  $T \gg T_g$ . These results, with  $\omega_D = 3.2 \times 10^{12}$  rad/s and  $K = 1.8 \times 10^{-27}$  s<sup>2</sup>, are represented by the curves corresponding to the three lowest temperatures in Figure 1. The fit of Equations (2), (3), and (5) to the simulation data is satisfactory, noting that the oscillations in the latter are an artefact of the finite size of the simulation box (Lewis and Wahnström, 1994). In Figure 2 are displayed (solid symbols) the best fit values for  $C_{\text{pho}}(t \rightarrow \infty; Q, T, )$  to the three lowest temperatures and absolute zero.

At higher temperatures, approaching the glass transition temperature of OTP, relaxation transpires, and the correlation function is no longer the simple product

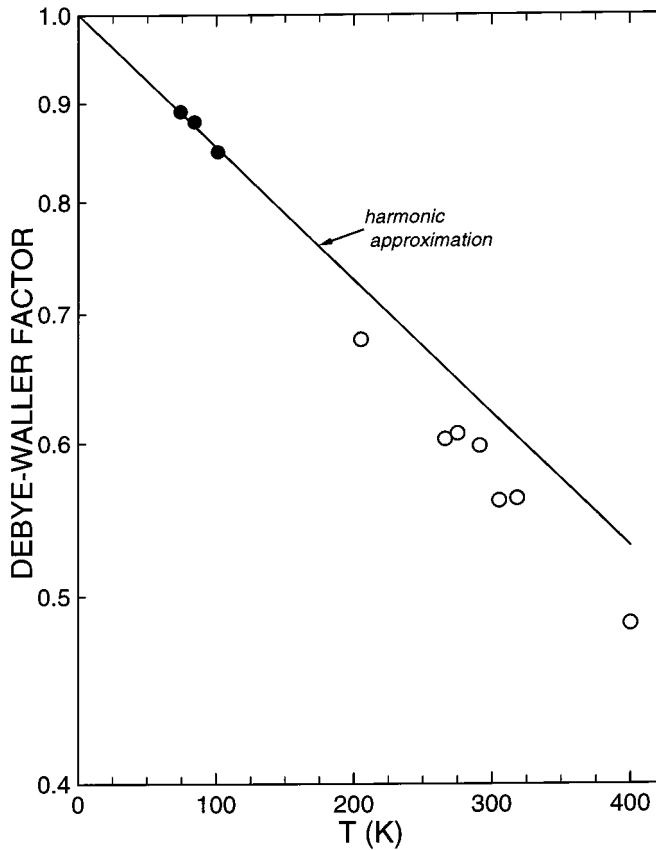


Figure 2. The long time limiting value of the phonon correlation function determined from fitting low (●●●) and high temperature (○○○) simulation data. The solid line represents extrapolation of the low temperature values, for which  $C_{\text{rel}}(t; Q, T)$  is unity. The actual  $C_{\text{pho}}(t \rightarrow \infty; Q, T)$  lie below this line, reflecting anharmonicity of the vibrational motions of OTP.

of a constant (i.e.,  $C_{\text{rel}}(t; Q, T) = 1$ ) times the phonon function. Without deconvolution of the vibrational and relaxation components, no rigorous interpretation of experimental data is possible (Ngai and Roland, 1997a). A simple expedient is to use Equation (3) to extrapolate the lower temperature results. Although this “harmonic approximation” has been used previously (Colmenero et al., 1993, 1994; Zorn et al., 1995; Ngai et al., 1995) to give at least qualitatively satisfactory results, it is clear (see, for example, Kartini et al., 1996) that deviation of the DWF from the low temperature behavior can be expected above  $T_g$ . The error inherent to the use of the harmonic approximation can be shown to be relatively small (Ngai and Roland, 1997c); nevertheless, there is uncertainty in any extrapolation of  $C_{\text{pho}}(t; Q, T)$  to very high temperatures. Accordingly, for higher temperatures we take the mag-

nitude of the DWF to be a parameter adjusted to improve agreement between calculation and experiment.

To describe the relaxation process prevailing at elevated temperatures, we use the coupling model. The model assumes relaxation is initially intermolecularly non-cooperative. This means the relaxational correlation function can be described as Debye relaxation

$$C_{\text{rel}}(t; Q, T) = \exp - \left( \frac{t}{\tau_0} \right). \quad (6)$$

In condensed matter, intermolecular interactions build up over time, resulting in unbalanced torques and forces being exerted on the relaxing species. According to the coupling model, this causes a transition from the initially uncorrelated motion to intermolecularly cooperative dynamics at long times. A form for the correlation function when intermolecularly cooperativity (“crowding coupling”) is manifested is

$$C_{\text{rel}}(t; Q, T) = \exp - \left( \frac{t}{\tau^*} \right)^\beta. \quad (7)$$

The stretch exponent  $\beta$  is related to the coupling parameter,  $n$ , as  $\beta = 1 - n$ , where  $n$  is a measure of the strength of the intermolecular constraints. Strong (weak) crowding coupling implies larger (smaller)  $n$ , within the bounds  $0 < n < 1$ . The coupling model assumes that the transition from Equation (6) to Equation (7) occurs at a temperature insensitive time  $t = t_c$ . Continuity of these two equations then yields

$$\tau^* = (t_c^{\beta-1} \tau_0)^{1/\beta}. \quad (8)$$

Equation (8) represents the most important result of the model, in that it enables the non-cooperative relaxation time prevailing at short times ( $t < t_c$ ) to be calculated from knowledge of the macroscopic relaxation time,  $\tau^*$ . Generally, only the latter can be directly obtained from experiment. Much use has been made of Equation (8) in predicting and accounting for the time and temperature dependencies of polymers and other glass-forming liquids (Böhmer et al., 1991; McGrath et al., 1992, 1995; Ngai and Platzek, 1995; Ngai and Roland, 1993a, 1993b, 1995; Ngai et al., 1992; Roland 1994, 1995; Roland and Ngai, 1991, 1992a, 1992b; Roland et al., 1994, 1996; Santangelo et al., 1993).

The higher temperature OTP data were fitted to Equations (1–8) by variation of the parameters  $K$  (i.e., the DWF),  $\beta$  and  $\tau_0$ . The latter values in turn determine  $\tau^*$  via Equation (8). The crossover time, at which the relaxation transitions from simple (Equation (6)) to stretched exponential (Equation (7)), is known experimentally (Colmenero et al., 1993, 1994; Ngai et al., 1995; Roland and Ngai, 1996) to be in the range of picoseconds. We choose  $t_c = 2 \times 10^{-12}$  s, recognizing the shape of  $C(t; Q, T)$  to be insensitive to small changes in the value of the crossover time.

Table I. Fitting parameters for OTP density-density correlation function.

$T$ (K)	Debye–Waller Factor	$\tau^*$ (psec)	$\beta$
74	0.891	–	–
84	0.880	–	–
101	0.849	–	–
205	0.679	–	–
266	0.603	5000	0.50
275	0.607	320	0.52
291	0.598	98	0.55
305	0.560	57	0.58
318	0.562	15	0.625
400	0.484	3.4	0.75

Displayed in Figure 1 are the fits of Equations (1), (2), and (5–8) to the density-density correlation function of OTP for temperatures at which relaxation contributes. The values of the DWF,  $C_{\text{pho}}(t \rightarrow \infty; Q, T, )$ , cooperative relaxation times,  $\tau^*$ , and the stretch exponents,  $\beta$ , are listed in Table I. In Figure 2 the best-fit DWF (hollow symbols) are compared to the harmonic approximation (extrapolation of Equation (3)), which predicts a linear relationship between the logarithm of the DWF and temperature. The actual DWF are lower, reflecting anharmonicity of the vibrations; that is, the amplitude of OTP’s phonon motions increases with increasing temperature more than that of a harmonic oscillator.

In Figure 3 the temperature-dependence of the non-cooperative relaxation times,  $\tau_0$ , is shown to be approximately Arrhenius, with an activation energy equal to 3.9 kcal/mole. This behavior is quite different from that of  $\tau^*$ , which herein, as well as generally, exhibits a Vogel–Fulcher (or WLF) temperature dependence (Ferry, 1980)

#### MODE COUPLING THEORY ANALYSIS

We now carry out a mode coupling theory analysis of the OTP data described in the previous section. According to mode coupling theory, the dynamic susceptibility should obey the scaling law (Götze, 1992)

$$\chi''(\omega) = |\chi''_{\min}|^{1/2} \chi''(\omega/\omega_{\min}), \quad (9)$$

in which  $\chi''_{\min} \propto (T - T_c)^{1/2a}$  and  $\omega_{\min} \propto |T_c - T|^{2a}$ . The quantities  $a$  and  $b$  are material dependent parameters of the theory. The dynamic susceptibility can be calculated from the transform of the structure factor data in Figure 1

$$\chi''(\omega) = \frac{\omega}{2\pi} \int_0^{\infty} C(t) \cos(\omega t) dt. \quad (10)$$

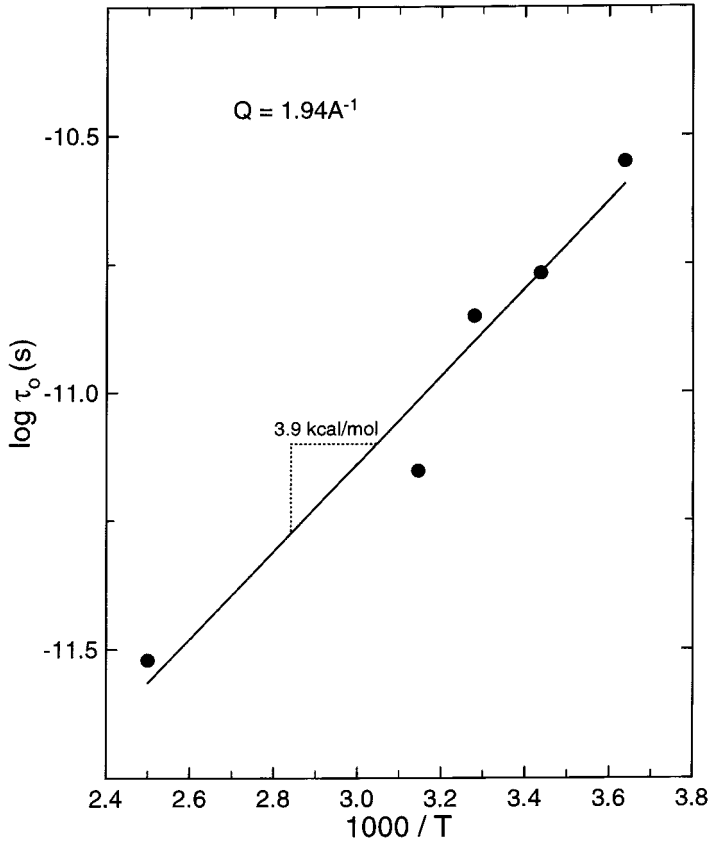


Figure 3. Non-cooperative relaxation times determined from fitting the data in Figure 1, yielding the indicated value of the activation energy for OTP.

We construct a mastercurve by scaling the susceptibility curves for each temperature both horizontally and vertically, in order to superimpose the minima (Equation (9)). As seen in Figure 4, the superpositioning is mediocre for frequencies more than a factor of 2 away from minimum. The mode coupling theory exponents  $a$  and  $b$  are then obtained by fitting the data in Figure 4 to the interpolation formula (Götze, 1992; Wuttke et al., 1994; Li et al., 1992a, 1992b)

$$\chi''(\omega) = \chi''_{\min} [b(\omega/\omega_{\min})^a + a(\omega_{\min}/\omega)^b] / (a + b). \quad (11)$$

These exponents are not freely adjustable, but rather are related according to

$$\lambda = \Gamma^2(1 - a) / \Gamma^2(1 - 2a) = \Gamma^2(1 + b) / \Gamma(1 + 2b), \quad (12)$$

where  $\Gamma$  represents the gamma function. As seen by the solid line in Figure 4, the low frequency side of  $\chi''(\omega)/\chi''_{\min}$  is well described by Equation (11); however, there is substantial deviation on the high frequency side of the peak. The obtained

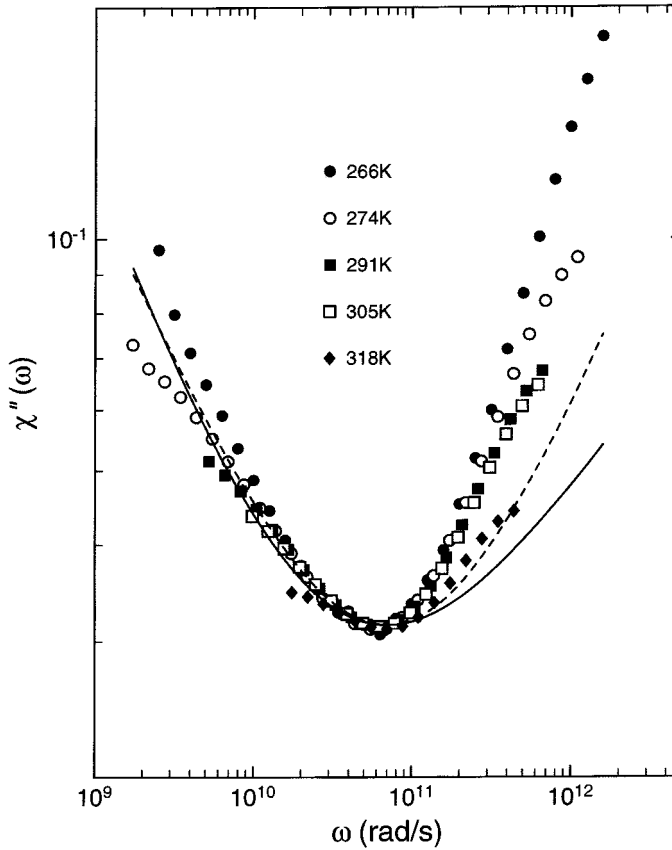


Figure 4. OTP susceptibility mastercurve in the vicinity of the minimum, calculated from the transform of the data in Figure 1. The solid line is the fit to Equation (11) with the constraint of Equation (12), yielding  $a = 0.30$  and  $b = 0.55$  for these parameters of mode coupling theory. Neglecting this constraint, the best-fit to Equation (11) (dashed line) yields  $a = 0.45$  and  $b = 0.50$ .

values for the exponents are  $a = 0.30$  and  $b = 0.55$ . If we let these parameters  $a$  and  $b$  be freely adjustable (i.e., neglecting the adherence to Equation (12) required by mode coupling theory), the resulting best-fit values of  $a = 0.45$  and  $b = 0.50$  only somewhat improve the fitting.

Mode coupling theory predicts a dynamic singularity at the critical temperature  $T_c$ . For temperatures above  $T_c$ , the theory makes the following predictions about the scaling of the susceptibility

$$(T - T_c)^{1/2} \propto \frac{\chi''_{\min}}{\omega_{\min}^a}. \quad (13)$$

In Figure 5 we plot the values deduced for  $\chi''_{\min}$  (Figure 4) versus temperature, obtaining a straight line (dashed curve) whose intercept gives  $T_c = 267$  K. This



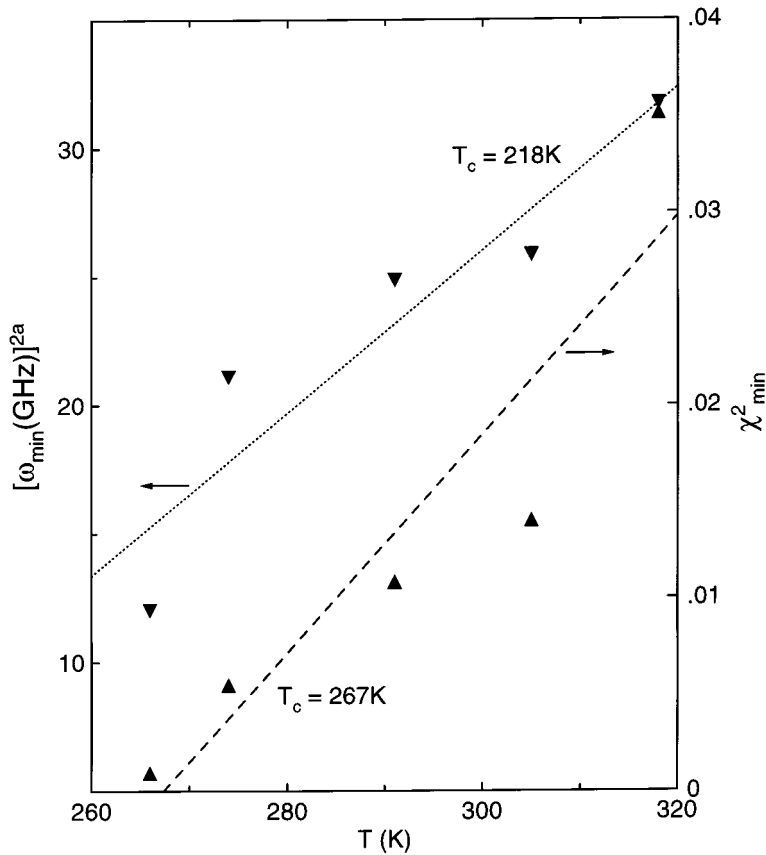


Figure 5. Temperature dependence of  $(\omega_{\min})^{2a}$  (▼▼▼) and of  $(\chi_{\min})^2$  (▲▲▲), using for the former the value of the exponent,  $a = 0.30$ , determined from the constrained fit (Equations (11) and (12)) in Figure 4. Extrapolation yields the indicated values of mode coupling theory's critical temperature ("dynamic singularity") for OTP.

result is close to the value deduced from the temperature dependence of the DWF (Lewis and Wahnström, 1994). On the other hand, a plot of  $\omega_{\min}^2$  versus temperature (dotted line in Figure 5) extrapolates to a critical temperature of 218 K. This contradicts the  $T_c$  obtained from the  $\chi_{\min}^2$  as well as being below  $T_g$ . Thus, the mode coupling theory approach does not give a self-consistent analysis of the OTP data.

The susceptibility minima curves in Figure 4 are qualitatively similar to quasi-elastic neutron scattering results for OTP (Petry et al., 1991; Kiebel et al., 1992). A analysis of the latter using mode coupling theory was carried out; however, the limitations of the data and/or of the theory prevented self-consistent values to be deduced for the parameters  $a$ ,  $b$ , and  $T_c$ . We also point out that the present failings of mode coupling theory – that is, the poor scaling in Figure 4 and the inconsistent

determinations of  $T_c$  in Figure 5 – mimic those seen in neutron and light scattering of glycerol (Wuttke et al., 1994) and light scattering on  $B_2O_3$  (Brodin et al., 1996). In the case of glycerol, deviations between experiment and mode coupling theory were tentatively ascribed to the network character of the hydrogen bonded liquid; for OTP, however, recourse cannot be made to such an explanation. An obvious inference from Figures 4 and 5 and these previous results is that approximate conformance of experimental data to scaling laws cannot serve as verification of mode coupling theory.

## VISCOSITY

We expect the short time density-density fluctuations, as revealed here from molecular dynamics simulation data, to underlie other dynamic variables, both microscopic (molecular length scale) and macroscopic (conventional spectroscopic frequencies); that is, there should be a connection between the short and long time properties. A commonly measured macroscopic dynamic variable is the shear viscosity,  $\eta$ . In the manner detailed above for density fluctuations, according to the coupling model the viscous relaxation can be decomposed into a fast process

$$C_\eta(t) = \exp - \left( \frac{t}{\tau_{0\eta}} \right) \quad (14)$$

for  $t < t_c$ , and an intermolecularly retarded process

$$C_\eta(t) = \exp - \left( \frac{t}{\tau_\eta^*} \right)^{1-n_\eta} \quad (15)$$

for  $t > t_c$ . Very often the Stokes–Einstein relation,  $\tau(T) \propto \eta(T)/T$  (Vilgis, 1994), is used to relate the respective temperature dependencies of the structural relaxation time and the viscosity. However, the length scale (or  $q$ -dependence) associated with the two quantities is by no means the same, calling into question the validity of such a relation. Instead we can compare the activation energy determined for the non-cooperative relaxation time  $\tau_0$  at  $Q = 1.94^{-1} \text{ \AA}^{-1}$  (Figure 3) directly with the temperature dependence of the viscosity. To be valid, the latter must correspond to time scales coinciding with that of  $\tau_0$ ; i.e., be less than the crossover time of a few picoseconds.

The viscosity of OTP has been reported over a wide range of values, with  $\eta$  reaching as low as  $10^{-4}$  Pa-s (Friz et al., 1968; Greet and Magill, 1967). The temperature dependence of the viscosity is displayed in Figure 6, indicating near Arrhenius behavior above about 500 C. From the asymptotic slope of Figure 6, we deduce an apparent activation energy of 4.3 kcal/mole. This is approximately equal to that determined above (Figure 3) for the non-cooperative relaxation process,  $E_A = 3.9$  kcal/mole.

This near equivalence of the respective activation energies for density fluctuations and the viscosity can be reconciled from the coupling model. We make use

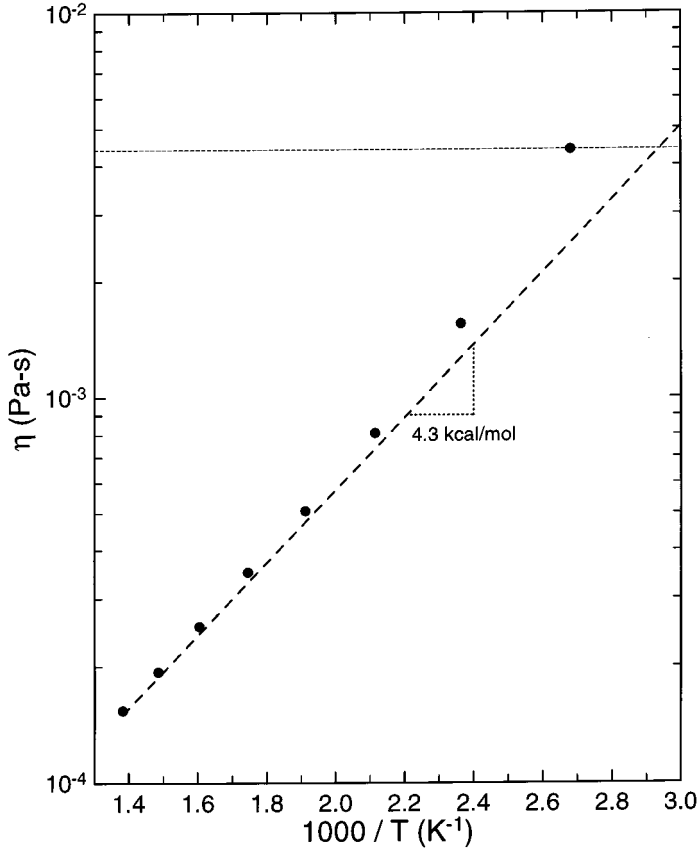


Figure 6. Viscosity of OTP (taken from Vilgis, 1994; Friz et al., 1968), whose limiting high temperature behavior yields an activation energy equal to 4.3 kcal/mole. The horizontal dashed lined denotes the viscosity for which  $\langle \tau_\eta \rangle = 2$  picoseconds (based on the Maxwell relation). This time corresponds to the crossover time,  $t_c$ , for the onset of intermolecular cooperativity.

of the Maxwell relation,  $\eta = G_\infty \langle \tau_\eta \rangle$ , to estimate the viscosity relaxation time, defined as

$$\langle \tau_\eta \rangle = \int_0^\infty C(t) dt. \quad (16)$$

Ignoring the weak temperature dependence of OTP's glassy modulus, we take a value of  $G_\infty = 2.2 \times 10^9$  Pa (Plazek et al., 1994), and calculate an average viscosity relaxation time. The horizontal dashed line in Figure 6 corresponds to the viscosity for which  $\langle \tau_\eta \rangle = 2$  ps; hence, below this line, the  $\langle \tau_\eta \rangle$  are less than  $t_c$ , the crossover time of the coupling model. Under this circumstance, the fast viscous relaxation (Equation (14)) dominates the viscous response, whereby  $\langle \tau_\eta \rangle$  is well approximated by  $\tau_{0\eta}$ . Since both  $\tau_{0\eta}$  and  $\tau_0$  for density fluctuations are (by

definition) free of cooperative effects, their activation energies should be nearly the same. The fact that this is indeed the case (cf. Figures 3 and 6) demonstrates a consistency between the fast dynamics of density fluctuations, as analyzed using the coupling model, and the viscosity at high temperatures.

This situation appears to be a general feature of glass-forming liquids. For example, in both glycerol (Roland and Ngai, 1997) and methanol (Ngai and Roland, 1997b),  $\tau_0$  for density fluctuations deduced from the short time data is found to have the same activation energy as the shear viscosity, when the latter is measured at temperature sufficiently high that  $\langle\tau_\eta\rangle$  is of the order of picoseconds. Thus, the coupling model provides a theoretical bridge between the macroscopic properties commonly probed by experimentalists and the short-time dynamics, which are of fundamental import.

## References

- Böhmer, R., Ngai, K.L., Angell, C.A. and Plazek, D.J., 'Nonexponential relaxation in strong and fragile glass formers', *Chem. Phys.* **94**, 1991, 3018–3026.
- Brodin, A., Engberg, D., Torell, L.M., Börjesson, L. and Sokolov, A.P., 'Non-monotonous temperature evolution of the glass transition dynamics in a strong glass former  $B_2O_3$ ', *Phys. Rev. B* **23**, 1996, 11511–11520.
- Colmenero, J., Arbe, A. and Alegría, A., 'Crossover from Debye to non-Debye dynamical behavior of the  $\alpha$ -relaxation observed by quasielastic neutron scattering in a glass-forming polymer', *Phys. Rev. Lett.* **71**, 1993, 2603–2606.
- Colmenero, J., Arbe, A. and Alegría, A., 'The dynamics of the alpha and beta relaxations in glass-forming polymers studied by quasielastic neutron scattering and dielectric spectroscopy', *J. Non-Cryst. Solids* **172–174**, 1994, 126–137.
- Ferry, J.D., *Viscoelastic Properties of Polymers*, Wiley, New York, 1980.
- Friz, G. et al., 1968, 'High temperature viscosity of liquids', *Atom Kernenergie* **13**, 1968, 25–29.
- Götze, W., 'Aspects of structural glass transition', in *Liquids, Freezing and the Glass Transition*, J.P. Hansen, D. Levesque and J. Zinn-Justin (eds), North-Holland, Amsterdam, 1991, 287–322.
- Götze, W. and Sjögren, L., 'Mode coupling theory of structural glass transition', *Rep. Prog. Phys.* **55**, 1992, 241–325.
- Greet, R.J. and Magill, J.H., 'An empirical corresponding-states relationship for liquid viscosity', *J. Phys. Chem.* **71**, 1967, 1746–1752.
- Kartini, E., Collins, M.F., Collier, B., Mezei, F. and Svensson, E.C., 'Inelastic-neutron-scattering studies on glassy and liquid  $Ca_{0.4}K_{0.6}(NO_3)_{1.4}$ ', *Phys. Rev. B* **54**, 1996, 6292–6300.
- Kiebel, M., Bartsch, E., Debus, O., Fujara, F., Petry, W. and Silesco, H., 'Secondary relaxation in the glass-transition regime of ortho-terphenyl observed by incoherent neutron scattering', *Phys. Rev. A* **45**, 1992, 10301–10306.
- Kittel, C., *Quantum Theory of Solids*, Wiley, New York, 1963, Chapter 19.
- Lewis, L.J. and Wahnström, G., 'Molecular-dynamics study of supercooled ortho-terphenyl', *Phys. Rev. E* **50**, 1994, 3865–3872.
- Li, G., Du, W.M., Sakai, A. and Cummins, H.Z., 'Light scattering investigation of alpha and beta relaxation near the liquid-glass transition of the molecular glass salol', *Phys. Rev. A* **46**, 1992a, 3343–3354.
- Li, G., Du, W.M., Chen, X.K. and Cummins, H.Z., 'Testing mode-coupling predictions for alpha and beta relaxation in  $Ca_{0.4}K_{0.6}(NO_3)_{1.4}$  near the liquid-glass transition by light scattering', *Phys. Rev. A* **45**, 1992b, 3867–3879.
- McGrath, K.J., Ngai, K.L. and Roland, C.M., 'Temperature dependence of segmental motion in polyisobutylene and poly(vinylethylene)', *Macromolecules* **25**, 1992, 4911–4914.
- McGrath, K.J., Ngai, K.L. and Roland, C.M., 'A comparison of segmental dynamics in polymers by  $^{13}C$  NMR spectroscopy', *Macromolecules* **28**, 1995, 2825–2830.

- Ngai, K.L., 'Universal patterns of relaxations in complex correlated systems', in *Disorder Effects on Relaxational Processes*, R. Richert and A. Blumen (eds), Springer-Verlag, Berlin, 1994, 89–150.
- Ngai, K.L. and Plazek, D.J., 'Identification of different modes of molecular motion in polymers that cause thermorheological complexity', *Rubber Chem. Technol.* **68**, 1995, 376–434.
- Ngai, K.L. and Roland, C.M., 'Intermolecular cooperativity and the temperature dependence of segmental relaxation in semicrystalline polymers', *Macromolecules* **26**, 1993a, 2688–2690.
- Ngai, K.L. and Roland, C.M., 'Chemical structure and intermolecular cooperativity: Dielectric relaxation results', *Macromolecules* **26**, 1993b, 6824–6830.
- Ngai, K.L. and Roland, C.M., 'Component dynamics in poly(vinylethylene)/polyisoprene blends', *Macromolecules* **28**, 1995, 4033–4035.
- Ngai, K.L. and Roland, C.M., 'Comment on depolarized light scattering study of molten zinc chloride', *Phys. Rev. E* **54**, 1996, 6969–6971.
- Ngai, K.L. and Roland, C.M., 'Comment on fast dynamics of glass-forming glycerol', *Phys. Rev. E* **55**, 1997a, 2069–2070.
- Ngai, K.L. and Roland, C.M., 'Short-time relaxational dynamics of the 'strong' glass-former methanol', *J. Phys. Chem.* **101**, 1997b, 3331–4437.
- Ngai, K.L. and Roland, C.M., 'Fast dynamics in glass-formers: Relation to fragility and the Kohlrausch exponent', in *Glasses and Glass Formers: New Results*, Mat. Res. Soc. Symp. Proc. Ser., C.A. Angell, K.L. Ngai, T. Egami, J. Kieffer and G.U. Nienha (eds), 1997c, 81–90.
- Ngai, K.L., Roland, C.M., O'Reilly, J.M. and Sedita, J.S., 'Trends in the temperature dependency of segmental relaxation in TMPC/PS blends', *Macromolecules* **25**, 1992, 3906–3909.
- Ngai, K.L., Roland, C.M. and Greaves, G.N., 'An interpretation of quasielastic neutron scattering and molecular dynamics simulation results on the glass transition', *J. Non-Cryst. Solids* **182**, 1995, 172–179.
- Petry, W., Bartsch, E., Fujara, F., Kiebel, M., Sillescu, H. and Farago, B., 'Dynamic anomaly in the glass transition region of orthoterphenyl', *Z. Phys. B* **83**, 1991, 175–182.
- Plazek, D.J., Bero, C.A. and Chay, I.-C., 'The recoverable compliance of amorphous materials', *J. Non-Cryst. Solids* **172–174**, 1994, 181–190.
- Roland, C.M., 'Constraints on local segmental motion in poly(vinylethylene) networks', *Macromolecules* **27**, 1994, 4242–4247.
- Roland, C.M., 'Mechanical and dielectric spectroscopy of aroclor, 1,2-polybutadiene, and their mixtures', *Macromolecules* **28**, 1995, 3463–3467.
- Roland, C.M. and Ngai, K.L., 'Dynamical heterogeneity in a miscible polymer blend', *Macromolecules* **24**, 1991, 2261–2265.
- Roland, C.M. and Ngai, K.L., 'Segmental relaxation and the correlation of time and temperature dependencies in PVME/polystyrene mixtures', *Macromolecules* **25**, 1992a, 363–367.
- Roland, C.M. and Ngai, K.L., 'Normalization of the temperature dependence of segmental relaxation times', *Macromolecules* **25**, 1992b, 5765–5768.
- Roland, C.M. and Ngai, K.L., 'Short time dynamics of glass forming liquids', *J. Chem. Phys.* **103**, 1995, 1152–1159.
- Roland, C.M. and Ngai, K.L., 'The anomalous Debye–Waller factor and the fragility of glasses', *J. Chem. Phys.* **104**, 1996, 2967–2970.
- Roland, C.M. and Ngai, K.L., 'Short-time viscous and density relaxation in glycerol and orthoterphenyl', *J. Chem. Phys.* **106**, 1997, 1187–1190.
- Roland, C.M., Santangelo, P.G., Baram, Z. and Runt, J., 'Segmental relaxation in blends of polychloroprene and epoxidized polyisoprene', *Macromolecules* **27**, 1994, 5382–5386.
- Roland, C.M., Ngai, K.L. and Lewis, L.J., 'High frequency relaxation of o-terphenyl', *J. Chem. Phys.* **103**, 1995, 4632–4636.
- Roland, C.M., Bero, C.A., Ngai, K.L. and Antonietti, M., 'Segmental relaxation in crosslinked rubber', in *Electrically Based Microstructural Characterization*, Mater. Res. Soc. Proc. Series, Vol. 411, 1996, 367–374.
- Santangelo, P.G., Ngai, K.L. and Roland, C.M., 'The distinctive manifestations of segmental motion in amorphous polytetrahydrofuran and polyisobutylene', *Macromolecules* **26**, 1993, 2682–2687.
- Tsang, K.Y. and Ngai, K.L., 'Relaxations in interacting arrays of oscillators', *Phys. Rev. E* **54**, 1996, R3067–3071.

- Vilgis, T.A., 'Models for transport and relaxation in glass forming and complex fluids: Universality?', in *Disorder Effects on Relaxational Processes*, R. Richert and A. Blumen (eds), Springer-Verlag, Berlin, 1994, 153–191.
- Wuttke, J., Hernandez, J., Li, G., Coddens, G., Cummins, H.Z., Fujara, F., Petry, W. and Sillescu, H., 'Neutron and light scattering study of supercooled glycerol', *Phys. Rev. Lett.* **72**, 1994, 3052–3056.
- Zorn, R., Arbe, A., J. Colmenero, B. Frick, D. Richter, and U. Buchenau, 'Neutron Scattering Study of the Picosecond Dynamics of Polybutadiene and Polyisoprene', *Phys. Rev. E* **52**, 1995, 781–795.